

Enhanced terahertz nonlinear response of GaAs by the tight field confinement in a nanogap ^{EP}

Cite as: APL Photonics **8**, 036107 (2023); <https://doi.org/10.1063/5.0134501>

Submitted: 11 November 2022 • Accepted: 20 February 2023 • Accepted Manuscript Online: 20 February 2023 • Published Online: 10 March 2023

 Dasom Kim,  Dai-Sik Kim and  Geunchang Choi

COLLECTIONS

 This paper was selected as an Editor's Pick



View Online



Export Citation



CrossMark

ARTICLES YOU MAY BE INTERESTED IN

[Complex nonlinear dynamics of polarization and transverse modes in a broad-area VCSEL](#)
APL Photonics **7**, 126108 (2022); <https://doi.org/10.1063/5.0104852>

[Polarization-mediated multi-state infrared system for fine temperature regulation](#)
APL Photonics **8**, 030801 (2023); <https://doi.org/10.1063/5.0136842>

[Parallel generation and coding of a terahertz pulse train](#)
APL Photonics **7**, 126105 (2022); <https://doi.org/10.1063/5.0123697>

APL Photonics

Applications Now Open for the
Early Career Editorial Advisory Board

[Learn more and submit!](#)

Enhanced terahertz nonlinear response of GaAs by the tight field confinement in a nanogap

Cite as: APL Photon. 8, 036107 (2023); doi: 10.1063/5.0134501
Submitted: 11 November 2022 • Accepted: 20 February 2023 •
Published Online: 10 March 2023



Dasom Kim,^{1,2,3}  Dai-Sik Kim,^{3,a)}  and Geunchang Choi^{4,a)} 

AFFILIATIONS

¹ Department of Electrical and Computer Engineering, Rice University, Houston, Texas 77005, USA

² Applied Physics Graduate Program, Smalley-Curl Institute, Rice University, Houston, Texas 77005, USA

³ Department of Physics, Ulsan National Institute of Science and Technology (UNIST), Ulsan 44919, Republic of Korea

⁴ School of Electrical and Electronics Engineering, Chung-Ang University, Seoul 06974, Republic of Korea

^{a)} Authors to whom correspondence should be addressed: daisikkim@unist.ac.kr and nightsky@cau.ac.kr

ABSTRACT

We demonstrated that an incident terahertz peak field amplitude below 0.01 MV/cm can trigger Zener tunneling in a semi-insulating GaAs. Moreover, a transmission decrease with an extinction ratio of 60% was observed in the semi-insulating GaAs with an electric field strength of up to 46 MV/cm (maximum incident peak field of ~ 0.29 MV/cm). These experimental results were realized by taking advantage of the nonlinear effects, such as Zener tunneling, impact ionization, and metal–insulator–metal tunneling in 5 nm metallic nanogaps on the GaAs; a strong field was locally confined in the vicinity of these gaps. The 5 nm gap enabled us to lower the voltage across the gap to suppress impact ionization while allowing Zener tunneling. Simulation results indicated that the effective thickness of the semiconductor increased as a function of the gap size. The approach used in this study decreases the threshold incident electric field for nonlinear responses as well as paves the way toward ultrathin high-speed electronic devices and ultrafast light pumps.

© 2023 Author(s). All article content, except where otherwise noted, is licensed under a Creative Commons Attribution (CC BY) license (<http://creativecommons.org/licenses/by/4.0/>). <https://doi.org/10.1063/5.0134501>

I. INTRODUCTION

Terahertz time-domain spectroscopy facilitates the study of carrier dynamics in semiconductors owing to its time-resolving ability with an ultrafast optical pump to excite carriers.^{1–3} During the last two decades, the development of intense terahertz pulse systems has allowed researchers to extend their work to the investigation of many-body interactions, such as electron–electron and electron–phonon scattering, through nonlinear terahertz response measurements.^{4–7} However, in the low frequency regime (0.1–3 THz), the generally achievable field strength is ~ 1 MV/cm in a Ti:sapphire amplified system with a 1 kHz repetition rate and in an electron accelerator with a 100 kHz repetition rate.⁸ Although the state-of-the-art strength reaches 6 MV/cm with a lower repetition rate,⁹ it is insufficient for fully studying the nonequilibrium many-body interactions.¹⁰ To reach such nonperturbative regimes, where an atomically strong electric field is required to induce interband tunneling,⁵ intervalley scattering,¹¹ or impact ionization,^{6,12} researchers have attempted to combine semiconductors with metamaterials.^{7,10,11,13}

Fabricating metamaterials, which confine and enhance an electric field in their vicinity, on the surface of GaAs enables the evaluation of the nonlinear phenomena. Such metamaterials show field-induced Zener tunneling¹⁴ and induce impact ionization near optical hotspots with an enhanced field of up to 30 MV/cm (the maximum incident peak field is 1.5 MV/cm).¹⁰ Further, nonlinear terahertz metamaterials that induce carrier generation have been reported for various applications.^{15–18} To achieve such nonlinear phenomena, amplified laser systems have been used to generate intense terahertz pulses,¹⁹ although these systems hamper the realization of extensive nonlinear applications.²⁰ Furthermore, such amplified laser systems are not feasible for use with other III–V semiconductors, whose bandgap energies are larger than that of GaAs because of their higher threshold fields (up to tens of MV/cm or higher). Therefore, generating a stronger electric field within an extremely confined volume is indispensable for researchers to study condensed matter in the terahertz frequency regime.

In this study, we induce a terahertz electric field of 46 MV/cm with the help of 5 nm-wide metal–insulator–metal structures on a

semi-insulating GaAs substrate. This field strength is far beyond the nonperturbative regime of GaAs and results in an unprecedented nonlinear transmission decrease with an extinction ratio of 60% owing to the field enhancement factor of the nanogaps. This narrow nanogap decreases the minimum incident peak field strength to 0.01 MV/cm for field-induced Zener tunneling in GaAs, thereby suppressing impact ionization. Moreover, we suggest the minimum semiconductor thickness required for the nonlinear response as a function of the gap size via simulations. The corresponding results indicate that the large field enhancement in the nanogap decreases the required semiconductor thickness.

II. RESULT AND DISCUSSIONS

Figures 1(a)–1(d) show the fabrication process of our 5 nm nanogap sample.²¹ First, a 100 nm-thick Au film is deposited by electron beam evaporation over a photoresist patterned on a semi-insulating GaAs (SI-GaAs, resistivity $\sim 10^8 \Omega\text{-cm}$) substrate. Rectangular holes [dimensions: $10 \mu\text{m}$ (l_x) \times $40 \mu\text{m}$ (l_y)] were exposed after the lift-off process. The pitch sizes of the hole arrays were $20 \mu\text{m}$ (p_x) and $50 \mu\text{m}$ (p_y) [Fig. 1(a)]. Second, a conformal coating of 5 nm alumina was performed by atomic layer deposition to ensure the formation of a dielectric layer on the sidewall of the metal [Fig. 1(b)]. Third, the same thickness of the metal was deposited on the alumina layer [Fig. 1(c)]. Finally, the excessive metal layer on the second floor was exfoliated using an adhesive tape to level the entire sample surface [Fig. 1(d)], and then, we obtained the vertically oriented insulating layer, resulting in a rectangular loop [Fig. 1(e)]. A cross-sectional scanning electron microscopic image of the 5 nm width (w) metal–insulator–metal structure is shown in Fig. 1(f).

Through a nanogap, only a polarized wave in the direction perpendicular to l_y is transmitted with a giant field enhancement.²² Further, it was proven that the enhancement rapidly decays along the light propagation axis.²³ As a result, nonlinear phenomena effectively occur in the vicinity of the nanogap.²⁴ In this work, the primarily occurring nonlinear phenomenon is field-induced Zener tunneling, which excites an electron, thereby resulting in a transmission decrease. This transmission decrease occurs when an atomically

strong field is induced to tilt the band structure, enabling an electron in the valence band to tunnel to the conduction band of a neighboring unit cell.^{10,25,26} Our nanogap sample shown in Fig. 1(f) mainly observes the local permittivity near itself,^{27,28} resulting in a decrease in the required semiconductor film thickness of interest down to nanometer size, which facilitates thin-film nonlinear applications.

We performed terahertz time-domain spectroscopy on the nanogaps and observed transmissions that depend on the incident field strength. For our terahertz transmission experiment, a single-cycle terahertz pulse was generated by a prism-cut lithium niobate (LiNbO_3) crystal via pulse-front-tilted optical rectification. A 1 kHz Ti:sapphire laser beam (central wavelength of 800 nm, pulse energy of 5.3 mJ, and pulse width of 35 fs; Spitfire, Spectra-Physics) was divided into terahertz generation and detection beams. The generated terahertz beam was guided by four off-axis parabolic mirrors. We controlled the incident terahertz field strengths from 3 to 360 kV/cm by using a pair of wire grid polarizers. Along with the 5 nm-gap sample, we also evaluated 2.5 μm - and 400 nm-gap samples fabricated by electron beam lithography. The corresponding results demonstrate the significant effect of the strong field enhancement in the nanogaps on the nonlinear responses of the material.

Figures 2(a) and 2(b) show the normalized transmitted amplitudes in the time domain for the 5 nm-gap and 2.5 μm -gap samples. To obtain the normalized transmitted amplitude, each transmitted amplitude of the sample in the time domain data is divided by the peak value of the transmitted amplitude of bare GaAs (500 μm thick) in the time domain data (supplementary material). For the frequency-domain analysis, we cut a transmitted pulse before the first echo arrived in the time domain. As the incident field strength increases, the 5 nm-gap sample shows drastically reduced normalized transmitted amplitudes in the time domain. By contrast, the 2.5 μm -gap sample shows a small change in the normalized transmitted amplitude over the entire time domain. Further, Figs. 2(c) and 2(d) present the transmission spectra (obtained by Fourier transformation of the time-domain measurements; see supplementary material for more details) of the 5 nm-gap and 2.5 μm -gap samples for incident field strengths ranging from

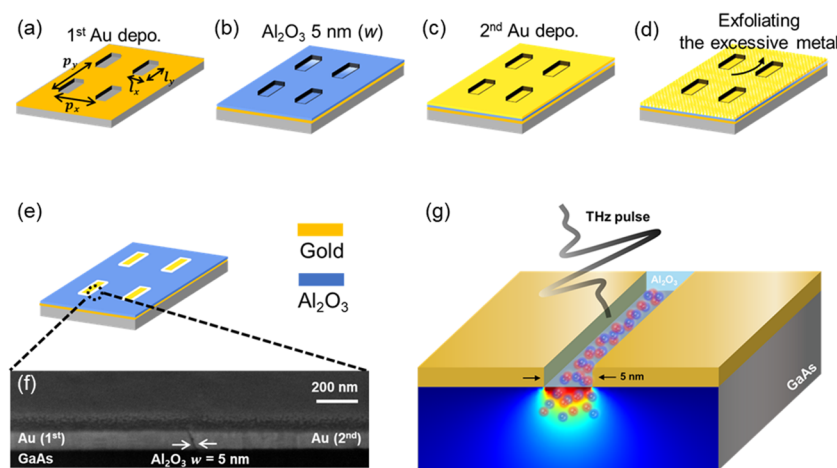


FIG. 1. (a)–(e) Schematic of the fabrication process for a 5 nm gap. Atomic layer deposition was used to fabricate the 5 nm gap. The white ring represents the 5 nm gap (Al_2O_3) between the first and second deposited gold layers. (f) Cross-sectional scanning electron microscopic image of a 5 nm-wide metal–insulator–metal gap on a GaAs substrate. (g) A terahertz wave illuminates a nanogap, in which the electric field is strongly enhanced so that an electron undergoes Zener tunneling through the tilted band structures; subsequently, the generated electrons participate in the impact ionization process.

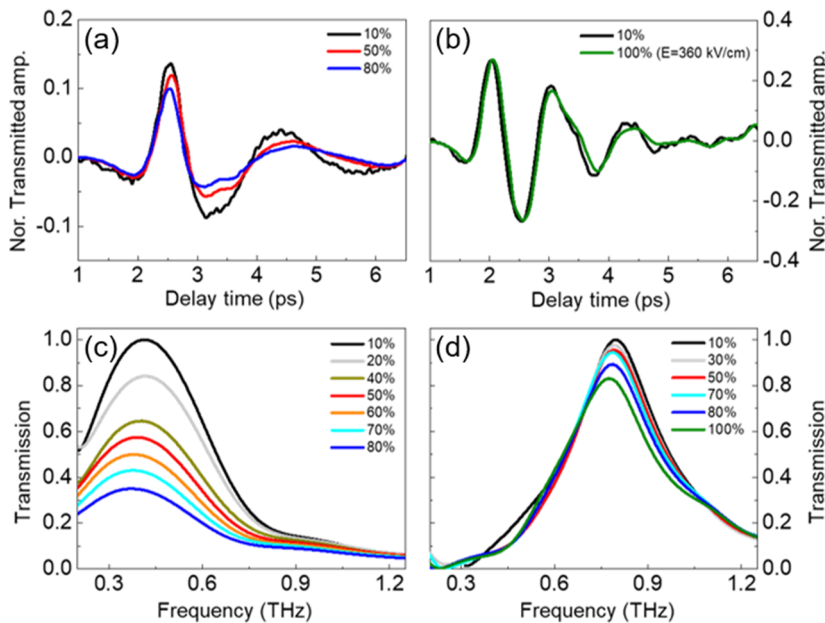


FIG. 2. Terahertz transmitted time traces of (a) the 5 nm gap and (b) the 2.5 μm gap normalized by their peak amplitudes at each field strength. The decrease in the amplitudes indicates carrier generation by the terahertz field in the vicinity of the gaps. Terahertz transmission of (c) the 5 nm gap and (d) the 2.5 μm gap; the transmission values are divided by the peak value at the minimum incident field. The transmission significantly drops at the peak amplitudes owing to the giant field enhancement at the peak frequency.

3.6 kV/cm to 0.36 MV/cm; the transmission values are divided by the peak value at the minimum incident field strength. In the frequency domain, significant nonlinear effects cause differences in the spectra, such as an extinction ratio of ~60% at 0.4 THz [Fig. 2(c)]. As the nonlinear effect becomes dominant, distinct redshifts are observed, which can be attributed to an increase in the effective index of the material around the gap.²⁹ For the 5 nm-gap sample, we restrict the incident field amplitude to 0.29 MV/cm because this nanogap sample can be damaged by a highly localized field and current around the gap when the field strength is 0.32 MV/cm.²⁹ Excited carriers increase the local index of refraction near the gap, and this high refractive index is responsible for the transmission decrease.²³ Materials that exhibit such responses can be applied to nonlinear switching devices with further parameter optimizations to increase the extinction ratio.

Figure 3(a) shows the time-integrated transmission of the 5 nm-, 400 nm-, and 2.5 μm-wide-gap samples; the corresponding values are normalized by the transmission T_0 at the minimum incident field (see supplementary material for details on the calculations of the transmission). The time-integrated transmission (T) is calculated using the relation: $T = \frac{\int E_{\text{sample}}^2(t) dt}{\int E_{\text{bare GaAs}}^2(t) dt}$, where E_{sample} and $E_{\text{bare GaAs}}$ are the transmitted time traces of the samples and a bare GaAs substrate, respectively.²⁹ The 5 nm-gap sample shows a large transmission decrease over the full range of the incident field strength, while the samples with wider gaps show a noticeable transmission decrease above a certain incident field strength, i.e., 150 and 275 kV/cm for the 400 nm-gap and 2.5 μm-gap samples, respectively. This result indicates that the strong field enhancement in the nanogap decreases the incident field strength required for the decrease in transmission due to nonlinear effects, and thus, without the field enhancement of the metamaterial, it is difficult to

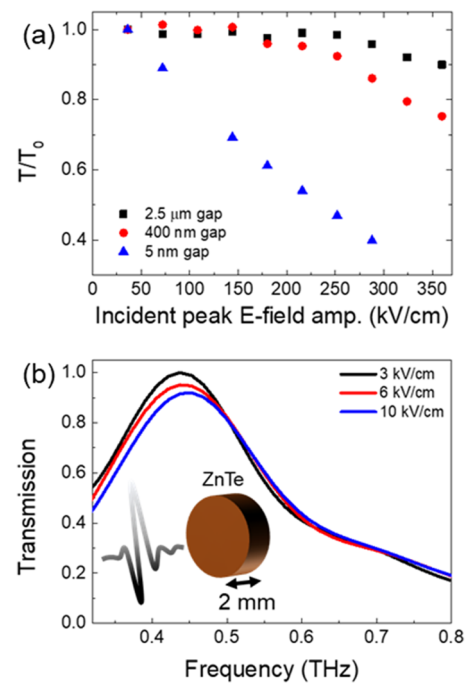


FIG. 3. (a) Time-integrated transmissions of the 5 nm- (blue triangles), 400 nm- (red circles), and 2.5 μm-wide-gap (black squares) samples; the corresponding values are normalized by the transmission T_0 at the minimum incident field. (b) Terahertz transmission measured with a 2 mm-thick ZnTe crystal for electro-optic sampling. The transmissions are divided by the peak value at the lowest incident field (3 kV/cm). The results reveal that an incident field strength of 6 kV/cm induces Zener tunneling.

observe a nonlinear effect via terahertz time-domain spectroscopy.³⁰ In the 5 nm-gap sample, the transmitted field strength decreases to ~40% of the reference field strength (i.e., in the absence of nonlinear effects) at the incident field amplitude of 300 kV/cm, indicating the largest transmission reduction observed among all samples.

To identify the incident electric field strength that induces nonlinear effects in the GaAs substrate, we systematically decreased the incident field strength [Fig. 3(b)]. For the terahertz electric field strength in the range of 3–10 kV/cm, a 2 mm-thick ZnTe crystal was used for the electro-optic sampling, which increased the signal-to-noise ratio. As evident from Fig. 3(b), the terahertz transmission starts to decline at an incident field of only 6 kV/cm, which implies that the threshold incident field for the 5 nm-gap sample is about 40 times lower than that of the 2.5 μ m-gap sample (275 kV/cm). This effective gap-induced drop in the transmission is a major breakthrough in research related to nonlinear phenomena induced by intense electric fields (~100 kV/cm). The presented metal-insulator-metal nanogap fabrication strategy enables the use of intermediate field strengths (~1 kV/cm) to induce nonlinear responses in semiconductors such as SI-GaAs.^{11,25,31} Although in our experiment, no decrease in the transmission was observed below 3 kV/cm (not shown), other measurement methods could be used to observe any nonlinear change. For instance, a terahertz-pump/optical-probe may reveal nonlinear responses due to the Franz-Keldysh effect.³²

For nonlinear response, the voltage applied across the gap for terahertz transmission is important. Figure 4 shows the time-integrated transmission (T/T_0) as a function of the voltage applied across the gaps for various antenna gap samples (see [supplementary material](#)). The voltage across the gap is estimated from the transient terahertz field strength measured at the output of the gap (more details can be found in the [supplementary material](#)). Notably, we found that a voltage of 23 V can result in a 60% transmission decrease, leading to Zener tunneling, which occurs when the applied electric field becomes sufficiently strong to tilt the band structure and allow a valence electron to tunnel through the potential barrier.¹⁴ These results demonstrate that several hundreds of voltages

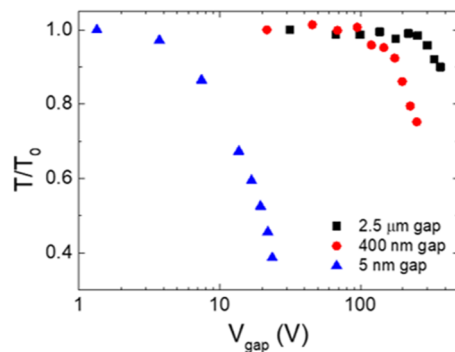


FIG. 4. Time-integrated transmissions of the 5 nm- (blue triangles), 400 nm- (red circles), and 2.5 μ m-wide-gap (black squares) samples, normalized by those of a GaAs bare substrate at each incident electric field strength, as functions of the gap voltage induced by the applied electric field.

are not required to control the transmission if a nanometer-sized gap is used. For an induced gap field that is responsible for the nonlinear effects, decreasing the gap width enables us to lower the voltage across the gap according to the equation: $E = V/w$, where V is the applied voltage and w is the gap width.

More importantly, the underlying mechanism is different from that observed in previous studies on nonlinear metamaterials, in which impact ionization can dominate over Zener tunneling when a strong electric field is applied.^{10,11} In our case, impact ionization is suppressed owing to the reduction in the active semiconductor area for carrier generation as the gap width decreases. On the contrary, Zener tunneling still occurs because of the enhanced terahertz electric field strength. To analyze the nonlinear effect in our case, the induced gap voltages corresponding to a 10% decrease in the terahertz transmission (from Fig. 4) of the antenna samples are compared. For a 10% transmission decrease, the gap voltages are ~7.5, 200, and 360 V for the 5 nm-, 400 nm-, and 2.5 μ m-gap samples, respectively. When the voltage across the 5 nm-gap is $V_{\text{gap}} = 7.5$ V, the electric field strength inside the gap is $E_{\text{gap}} = 1.5$ V/nm, which is sufficiently strong to induce Zener tunneling. Because the threshold energy for impact ionization in GaAs is 1.6 eV,¹⁰ $V_{\text{gap}} = 7.5$ V results in less than five ionization steps for a single electron, culminating in a carrier multiplication factor of $2^5 \approx 30$. In contrast to the 5 nm-gap sample, when the voltage across the 400 nm-gap is near the highest value of $V_{\text{gap}} = 200$ V, the electric field strength inside the gap becomes $E_{\text{gap}} = 0.5$ V/nm. This low field strength induces an extremely weak Zener tunneling but safely allows at least ten impact ionization steps, which result in a carrier multiplication factor of 1000 according to the previously reported results.^{10,25} Because of such a large carrier multiplication factor, a large number of carriers are expected to be generated, which can be limited when the number of generated carriers reaches the Pauli blocking regime. Therefore, we can assume that compared with the 2.5 μ m-gap and 400 nm-gap samples, the 5 nm-gap sample enables a significant decrease in the transmission with a low gap voltage and a small number of impact ionization steps.^{33–35} Although impact ionization is suppressed in the 5 nm gap, the extinction ratio of 60% shown in Fig. 4 originates from the large number of carriers generated by Zener tunneling and impact ionization. We note that the influence of the intervalley scattering or nonparabolicity effect on the transmission drop is insignificant due to the low initial carrier concentration ($\sim 10^7$ cm⁻³) in SI-GaAs.³⁶ However, an intense terahertz pulse generates free carriers in GaAs as well as enables metal-insulator-metal tunneling,³⁷ such as Fowler-Nordheim tunneling, in the nanogaps.²⁹ Nevertheless, the transmission decrease is not governed by the metal-insulator-metal tunneling because it begins above 2.5 V/nm, as demonstrated by the extinction shown by the 5 nm-gap on a quartz substrate (see [supplementary material](#)).

Finally, we analyze the interacting region, where the nonlinear phenomena occur, via simulations of the electric field amplitude distributions. Without the metamaterial-induced nonlinearity of the semiconductor substrate, the confined field near the gap is proportional to the gap size of the metamaterials.³⁸ Figure 5(a) presents the numerically simulated (COMSOL Multiphysics) field distributions of the terahertz waves for the 2.5 μ m-gap and 5 nm-gap samples. The corresponding electric field amplitudes, along the z -axis from the gap surface, for various incident field strengths are plotted in

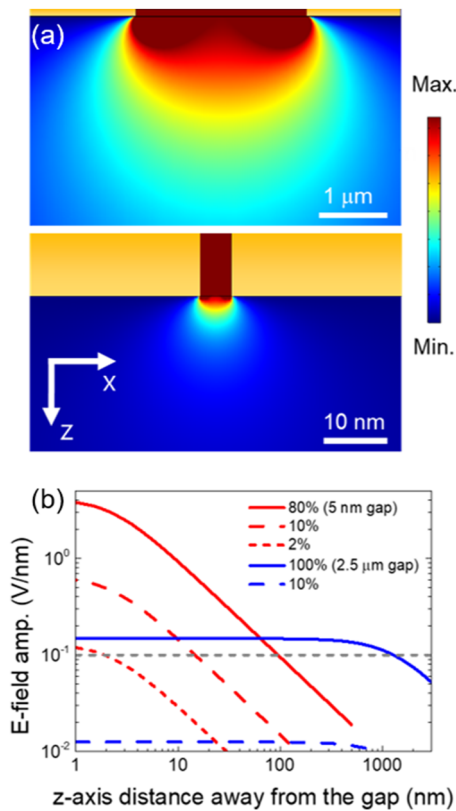


FIG. 5. (a) Electric field distributions (E_x) of the $2.5 \mu\text{m}$ (top) and 5 nm (bottom) gaps in the vicinity of the gaps, normalized by their maximum values. (b) Electric field amplitudes extracted from (a) along the z -axis from the center of the gap at the surface. The red and blue curves represent the distributions for the 5 nm and $2.5 \mu\text{m}$ gaps with different incident electric fields, respectively. The gray dashed line indicates the threshold field strength (0.1 V/nm) for Zener tunneling.

Fig. 5(b). The gray dashed line indicates a field strength of 0.1 V/nm with which tunneling rate in the SI-GaAs is above the order of $10^{10} \text{ (cm}^{-3} \text{ 100 fs}^{-1}\text{)}$ for Zener tunneling. This value surpasses the initial carrier density of the SI-GaAs substrate.¹⁰ While a field strength below 0.1 V/nm can still induce carrier generation by Zener tunneling, the terahertz transmission shows negligible changes because of the low generation rate. We note that, based on **Fig. 3(b)**, the minimum incident electric field strength required for decreasing the transmission is around 6 kV/cm , and the corresponding gap voltage is $0.08\text{--}0.17 \text{ V/nm}$. In the case of the 5 nm -gap, even the incident electric field strength of 6 kV/cm crosses the line indicating the limit. This field strength corresponds to a small change in the transmission spectrum shown in **Fig. 3(b)**. The region where Zener tunneling occurs is within 2 nm from the gap surface. As the input field strength increases, the interacting volume increases linearly (the electric field strength decays as the distance from the gap surface increases).³⁹ In the case of the $2.5 \mu\text{m}$ -gap sample, the field barely crosses the gray line and corresponds to a negligible change in the transmission spectra.

III. CONCLUSION

In summary, we demonstrated that Zener tunneling can be observed in GaAs with surface nanostructures under an electric field strength that is two orders of magnitude smaller than that required for the same semiconductor without a nanostructured surface. A narrow gap is more sensitive to the field confined within its volume than that outside. With the nanogap, we obtained a 60% decrease in transmission due to nonlinear effects, and this significant transmission decrease can be beneficial for nonlinear sensor applications. Furthermore, the interacting volume for a narrower gap is much smaller than that for a wider gap, and consequently, a narrower gap is more compatible with thin epitaxially-grown semiconductor films. The strategy presented in this paper will allow researchers, focused on the intermediate electric field strength regime ($\sim 1 \text{ kV/cm}$), to investigate unprecedented nonlinear phenomena. In addition, the proposed strategy has diverse potential applications with ultrathin semiconductors.

SUPPLEMENTARY MATERIAL

In the [supplementary material](#), details are provided about the estimation of the voltage across a gap induced by the transmitted terahertz pulse and metal-insulator-metal tunneling in a 5 nm gap. Calculation of the normalization process.

ACKNOWLEDGMENTS

This work was supported by the Chung-Ang University Research Grant in 2021 and the MSIT (Ministry of Science and ICT), Korea, under the ITRC (Information Technology Research Center) support program (No. IITP-2023-RS-2022-00156353) supervised by the IITP (Institute for Information & Communications Technology Planning & Evaluation). The authors thank Professor Junichiro Kono for discussions on terahertz-induced nonlinear effects.

AUTHOR DECLARATIONS

Conflict of Interest

The authors have no conflicts to disclose.

Author Contributions

Dasom Kim: Data curation (equal); Formal analysis (equal); Investigation (equal); Methodology (equal); Software (equal); Writing – original draft (equal). **Dai-Sik Kim:** Funding acquisition (supporting); Investigation (supporting); Project administration (supporting); Supervision (supporting). **Geunchang Choi:** Conceptualization (lead); Data curation (equal); Formal analysis (equal); Funding acquisition (lead); Investigation (equal); Methodology (equal); Project administration (lead); Software (equal); Writing – original draft (equal); Writing – review & editing (equal).

DATA AVAILABILITY

The data that support the findings of this study are available from the corresponding authors upon reasonable request.

REFERENCES

- ¹R. Ulbricht, E. Hendry, J. Shan, T. F. Heinz, and M. Bonn, "Carrier dynamics in semiconductors studied with time-resolved terahertz spectroscopy," *Rev. Mod. Phys.* **83**, 543–586 (2011).
- ²H. J. Joyce, C. J. Docherty, Q. Gao, H. H. Tan, C. Jagadish, J. Lloyd-Hughes, L. M. Herz, and M. B. Johnston, "Electronic properties of GaAs, InAs and InP nanowires studied by terahertz spectroscopy," *Nanotechnology* **24**, 214006 (2013).
- ³J. Hebling, M. C. Hoffmann, H. Y. Hwang, K.-L. Yeh, and K. A. Nelson, "Observation of nonequilibrium carrier distribution in Ge, Si, and GaAs by terahertz pump-terahertz probe measurements," *Phys. Rev. B* **81**, 035201 (2010).
- ⁴P. Gaal, K. Reimann, M. Woerner, T. Elsaesser, R. Hey, and K. H. Ploog, "Nonlinear terahertz response of *n*-type GaAs," *Phys. Rev. Lett.* **96**, 187402 (2006).
- ⁵W. Kuehn, P. Gaal, K. Reimann, M. Woerner, T. Elsaesser, and R. Hey, "Terahertz-induced interband tunneling of electrons in GaAs," *Phys. Rev. B* **82**, 075204 (2010).
- ⁶A. T. Tarekegne, K. Iwaszczuk, M. Zalkovskij, A. C. Strikwerda, and P. U. Jepsen, "Impact ionization in high resistivity silicon induced by an intense terahertz field enhanced by an antenna array," *New J. Phys.* **17**, 043002 (2015).
- ⁷A. T. Tarekegne, H. Hirori, K. Tanaka, K. Iwaszczuk, and P. U. Jepsen, "Impact ionization dynamics in silicon by MV/cm THz fields," *New J. Phys.* **19**, 123018 (2017).
- ⁸B. Zhang, Z. Ma, J. Ma, X. Wu, C. Ouyang, D. Kong, T. Hong, X. Wang, P. Yang, L. Chen, Y. Li, and J. Zhang, "1.4-mJ high energy terahertz radiation from lithium niobates," *Laser Photonics Rev.* **15**, 2000295 (2021).
- ⁹B. Green, S. Kovalev, V. Asgekar, G. Geloni, U. Lehnert, T. Golz, M. Kuntzsch, C. Bauer, J. Hauser, J. Voigtlaender, B. Wustmann, I. Koesterke, M. Schwarz, M. Freitag, A. Arnold, J. Teichert, M. Justus, W. Seidel, C. Ilgner, N. Awari, D. Nicoletti, S. Kaiser, Y. Laplace, S. Rajasekaran, L. Zhang, S. Winnerl, H. Schneider, G. Schay, I. Lorincz, A. A. Rauscher, I. Radu, S. Mährlein, T. H. Kim, J. S. Lee, T. Kampfrath, S. Wall, J. Heberle, A. Malnasi-Csizmadia, A. Steiger, A. S. Müller, M. Helm, U. Schramm, T. Cowan, P. Michel, A. Cavalleri, A. S. Fisher, N. Stojanovic, and M. Gensch, "High-field high-repetition-rate sources for the coherent THz control of matter," *Sci. Rep.* **6**, 22256 (2016).
- ¹⁰C. Lange, T. Maag, M. Hohenleutner, S. Baierl, O. Schubert, E. R. J. Edwards, D. Bougeard, G. Woltersdorf, and R. Huber, "Extremely nonperturbative nonlinearities in GaAs driven by atomically strong terahertz fields in gold metamaterials," *Phys. Rev. Lett.* **113**, 227401 (2014).
- ¹¹K. Fan, H. Y. Hwang, M. Liu, A. C. Strikwerda, A. Sternbach, J. Zhang, X. Zhao, X. Zhang, K. A. Nelson, and R. D. Averitt, "Nonlinear terahertz metamaterials via field-enhanced carrier dynamics in GaAs," *Phys. Rev. Lett.* **110**, 217404 (2013).
- ¹²R. D. Schaller and V. I. Klimov, "High efficiency carrier multiplication in PbSe nanocrystals: Implications for solar energy conversion," *Phys. Rev. Lett.* **92**, 186601 (2004).
- ¹³H. R. Seren, J. Zhang, G. R. Keiser, S. J. Maddox, X. Zhao, K. Fan, S. R. Bank, X. Zhang, and R. D. Averitt, "Nonlinear terahertz devices utilizing semiconducting plasmonic metamaterials," *Light: Sci. Appl.* **5**, e16078 (2016).
- ¹⁴E. O. Kane, "Zener tunneling in semiconductors," *J. Phys. Chem. Solids* **12**, 181–188 (1960).
- ¹⁵R. Rana, L. Balaghi, I. Fotev, H. Schneider, M. Helm, E. Dimakis, and A. Pashkin, "Nonlinear charge transport in InGaAs nanowires at terahertz frequencies," *Nano Lett.* **20**, 3225–3231 (2020).
- ¹⁶D. J. Ironside, R. Salas, P.-Y. Chen, K. Q. Le, A. Alú, and S. R. Bank, "Enhancing THz generation in photomixers using a metamaterial approach," *Opt. Express* **27**, 9481–9494 (2019).
- ¹⁷A. R. Wright, X. G. Xu, J. C. Cao, and C. Zhang, "Strong nonlinear optical response of graphene in the terahertz regime," *Appl. Phys. Lett.* **95**, 072101 (2009).
- ¹⁸I. Al-Naib, G. Sharma, M. M. Dignam, H. Hafez, A. Ibrahim, D. G. Cooke, T. Ozaki, and R. Morandotti, "Effect of local field enhancement on the nonlinear terahertz response of a silicon-based metamaterial," *Phys. Rev. B* **88**, 195203 (2013).
- ¹⁹B. J. Kang, D. Rohrbach, F. D. J. Brunner, S. Bagiante, H. Sigg, and T. Feurer, "Ultrafast and low-threshold THz mode switching of two-dimensional nonlinear metamaterials," *Nano Lett.* **22**, 2016–2022 (2022).
- ²⁰M. Liu, H. Y. Hwang, H. Tao, A. C. Strikwerda, K. Fan, G. R. Keiser, A. J. Sternbach, K. G. West, S. Kittiwatanakul, J. Lu, S. A. Wolf, F. G. Omenetto, X. Zhang, K. A. Nelson, and R. D. Averitt, "Terahertz-field-induced insulator-to-metal transition in vanadium dioxide metamaterial," *Nature* **487**, 345–348 (2012).
- ²¹X. Chen, H.-R. Park, M. Pelton, X. Piao, N. C. Lindquist, H. Im, Y. J. Kim, J. S. Ahn, K. J. Ahn, N. Park, D.-S. Kim, and S.-H. Oh, "Atomic layer lithography of wafer-scale nanogap arrays for extreme confinement of electromagnetic waves," *Nat. Commun.* **4**, 2361 (2013).
- ²²M. A. Seo, H. R. Park, S. M. Koo, D. J. Park, J. H. Kang, O. K. Suwal, S. S. Choi, P. C. M. Planken, G. S. Park, N. K. Park, Q. H. Park, and D. S. Kim, "Terahertz field enhancement by a metallic nano slit operating beyond the skin-depth limit," *Nat. Photonics* **3**, 152–156 (2009).
- ²³J. Jeong, H. S. Yun, D. Kim, K. S. Lee, H.-K. Choi, Z. H. Kim, S. W. Lee, and D.-S. Kim, "High contrast detection of water-filled terahertz nanotrenches," *Adv. Opt. Mater.* **6**, 1800582 (2018).
- ²⁴H.-T. Chen, W. J. Padilla, J. M. O. Zide, A. C. Gossard, A. J. Taylor, and R. D. Averitt, "Active terahertz metamaterial devices," *Nature* **444**, 597–600 (2006).
- ²⁵H. Hirori, K. Shinokita, M. Shirai, S. Tani, Y. Kadoya, and K. Tanaka, "Extraordinary carrier multiplication gated by a picosecond electric field pulse," *Nat. Commun.* **2**, 594 (2011).
- ²⁶C. Vicario, M. Shalaby, and C. P. Hauri, "Subcycle extreme nonlinearities in GaP induced by an ultrastrong terahertz field," *Phys. Rev. Lett.* **118**, 083901 (2017).
- ²⁷G. Choi, Y.-M. Bahk, T. Kang, Y. Lee, B. H. Son, Y. H. Ahn, M. Seo, and D.-S. Kim, "Terahertz nanoprobe of semiconductor surface dynamics," *Nano Lett.* **17**, 6397–6401 (2017).
- ²⁸D. Kim, J. Jeong, G. Choi, Y.-M. Bahk, T. Kang, D. Lee, B. Thusa, and D.-S. Kim, "Giant field enhancements in ultrathin nanoslots above 1 terahertz," *ACS Photonics* **5**, 1885–1890 (2018).
- ²⁹J.-Y. Kim, B. J. Kang, J. Park, Y.-M. Bahk, W. T. Kim, J. Rhie, H. Jeon, F. Rotermund, and D.-S. Kim, "Terahertz quantum plasmonics of nanoslot antennas in nonlinear regime," *Nano Lett.* **15**, 6683–6688 (2015).
- ³⁰Y.-G. Jeong, M. J. Paul, S.-H. Kim, K.-J. Yee, D.-S. Kim, and Y.-S. Lee, "Large enhancement of nonlinear terahertz absorption in intrinsic GaAs by plasmonic nano antennas," *Appl. Phys. Lett.* **103**, 171109 (2013).
- ³¹J. R. Danielson, Y.-S. Lee, J. P. Prineas, J. T. Steiner, M. Kira, and S. W. Koch, "Interaction of strong single-cycle terahertz pulses with semiconductor quantum wells," *Phys. Rev. Lett.* **99**, 237401 (2007).
- ³²F. Novelli, D. Fausti, F. Giusti, F. Parmigiani, and M. Hoffmann, "Mixed regime of light-matter interaction revealed by phase sensitive measurements of the dynamical Franz-Keldysh effect," *Sci. Rep.* **3**, 1227 (2013).
- ³³Y. Okuto and C. R. Crowell, "Energy-conservation considerations in the characterization of impact ionization in semiconductors," *Phys. Rev. B* **6**, 3076–3081 (1972).
- ³⁴Y. Okuto and C. R. Crowell, "Ionization coefficients in semiconductors: A nonlocalized property," *Phys. Rev. B* **10**, 4284–4296 (1974).
- ³⁵A. Spinelli, A. Pacelli, and A. L. Lacaita, "Dead space approximation for impact ionization in silicon," *Appl. Phys. Lett.* **69**, 3707–3709 (1996).
- ³⁶F. Blanchard, D. Golde, F. H. Su, L. Razzari, G. Sharma, R. Morandotti, T. Ozaki, M. Reid, M. Kira, S. W. Koch, and F. A. Hegmann, "Effective mass anisotropy of hot electrons in nonparabolic conduction bands of *n*-doped InGaAs films using ultrafast terahertz pump-probe techniques," *Phys. Rev. Lett.* **107**, 107401 (2011).
- ³⁷J. G. Simmons, "Generalized formula for the electric tunnel effect between similar electrodes separated by a thin insulating film," *J. Appl. Phys.* **34**, 1793–1803 (1963).
- ³⁸G. Choi, T. Kang, M. Seo, D.-S. Kim, and Y.-M. Bahk, "Enhanced surface carrier response by field overlapping in metal nanopatterned semiconductor," *ACS Photonics* **5**, 4739–4744 (2018).
- ³⁹J. Jeong, D.-S. Kim, and H.-R. Park, "Beyond-hot-spot absorption enhancement on top of terahertz nanotrenches," *Nanophotonics* **11**, 3159–3167 (2022).